Development of a Multilayer Urban Canopy Model Combined with a Ray Tracing Algorithm

Van Q. Doan* and Hiroyuki Kusaka
Center for Computational Sciences, University of Tsukuba, Japan

Abstract

This study introduces a new multiple-layer urban canopy model (MUCM) combined with a ray-tracing algorithm. In the model, we parameterize the urban morphology as an infinite array of identical three-dimensional buildings separated by roads. Heat exchanges are solved for each urban surface at each vertical layer. The ray-tracing scheme is used to explicitly calculate the view factors as well as both the sunlit and shadow fractions of the urban surfaces during the daytime. As a test, we show that this combined MUCM accurately models observations at Kugahara, Tokyo. Thus, the combined MUCM is a new tool for urban climate modelers to more realistically represent radiative processes on urban surfaces. In particular, it may contribute to our understanding of urban climate in the mega-cities of Asia, which generally have high-rise buildings that are more difficult to model with simpler radiative schemes.

(**Citation**: Doan, V. Q., and H. Kusaka, 2018: Development of a multilayer urban canopy model combined with a ray tracing algorithm. *SOLA*, **15**, 37−40, doi:10.2151/sola.2019-008.)

1. Introduction

Modeling the dynamic and thermodynamic effects of urban areas on the atmosphere can be done several ways. A popular method involves computational fluid dynamics (CFD) modeling to explicitly resolve the interaction of each urban structure and the air. However, CFD models are generally computational expensive to use. A simpler approach is the land surface model (LSM). The LSM was developed to couple with a mesoscale climate model to represent the bulk effect of urban areas. In a standard LSM, urban effects are represented through parameters such as roughness length, albedo, heat capacity, and thermal conductivity. This method is simple and effective, but unable to represent more-complex processes that are associated with the existence of buildings (Warner 2011).

Another method is the urban canopy model (UCM). In general, a UCM can more realistically represent buildings and urban canyons than a standard LSM, though they are still unable to directly resolve individual effects of urban structures like a CFD model. Concerning the types of UCMs, Grimmond et al. (2010, 2011) classified UCMs based on their parameterization of urban morphology, calculation of urban fluxes, and treatment of radiation reflections and street trees. Among these classification criteria, the most important is the method of parameterizing urban morphology.

In addition, urban canopy models can be broadly divided into single-layer and multi-layer models. Single-layer models have only one atmospheric layer in the urban canopy. A single-layer UCM (or SUMC) simplifies urban morphology to an urban canyon with a roof, wall, and road, allowing the model to include a radiative trapping effect and turbulent exchange within the urban canopy (e.g., Masson 2000; Kusaka et al. 2001; Harman et al. 2004; Best 2005; Kanda et al. 2005a; Krayenhoff et al. 2007; Lee and Park 2008; Oleson et al. 2008). In contrast, multi-layer models have several vertical layers within the canopy. The added layers allow one to explicitly represent the physical processes at each vertical layer. In particular, a multi-layer UCM (or MUCM) divides the urban canopy into a number of vertical layers, as well as divides the roof and road into a number of horizontal patches, each with their own parameter values and energy exchanges. Some models also allow for variable building height, or even differing roof, wall, and road characteristics (e.g., Brown 2000; Hagishima et al. 2001; Vu et al. 2002; Martilli et al. 2002; Dupont et al. 2004; Otte et al. 2004; Kondo et al. 2005; Salamanca et al. 2010). Unlike the SUCM, the MUCM can explicitly resolve vertical profiles of control variables such as air temperature, humidity, and windspeed within the urban canopy.

With the more explicit parameterization in MUCMs comes a greater need to accurately represent the radiative exchanges on and within urban surfaces. These exchanges are represented by the view factors, which are the fractions of the sky and other urban surfaces that are visible from a reference surface. In addition, the model should represent the changing sunlit ratio of each urban surface during the day that is essential for predicting the shortwave radiative flux exchanges. Most MUCMs have used simple analytical methods to approximate these view factors and to calculate the sunlit area (e.g., Kondo et al. 2005; Martilii et al. 2002; Ikeda and Kusaka 2010). Analytical methods are relatively easy to use and computationally less demanding due to using simplified analytical functions of building properties and sun positions. However, they are problematic when handling three dimensional urban canopies, and sometimes, tend to underestimate systematically the radiation trapping effect within the urban canopy layer (Kanda et al. 2005b). Here, we introduce the ray-tracing method to increase accuracy of these factors.

Ray tracing is a rendering method that can produce realistic lighting effects, often being used in computer graphics and architecture design. The method traces the path of light, and then simulates the way that the light interacts with visual objects. For UCMs, the method should provide better estimates than analytic approximations of the view factors as well as more accurate calculations of the sunlit and shadow areas. Previously, Aoyagi and Seino (2011) used a ray-tracing-like method for calculating the sky-view factor for their single-layer UCM. Here, we apply the ray-tracing method to a multi-layer UCM for both the view factors and the sunlit area calculation.

The combined MUCM can be a new option for urban climate modelers to represent more realistically the radiative processes on urban surfaces. For numerical urban climate studies of Asian cities, with their higher fraction of high-rise buildings over those in Europe, the use of such a multi-layer UCM may be particularly useful. Additionally, the ray-tracing is expected to be more powerful than the analytical approximation in the complex mixture with high- and low-rise buildings.

2. Description of the MUCM

The urban morphology is parameterized as an infinite array of solid three-dimensional buildings. The buildings and roads are identical, with the buildings' walls facing east, west, north, and south (Fig. 1). This structure is similar to that in Kondo et al. (2005) and Ikeda and Kusaka (2012). The model consists of multiple vertical layers, with the physical processes being solved for each urban surface at each layer.

For the green areas, we use a simple grass model. The grass

Corresponding author: Hiroyuki Kusaka, University of Tsukuba, 1-1-1 Tennodai, Tsukuba, 305-8577 Japan. E-mail: kusaka@ccs.tsukuba.ac.jp.
* Current affiliation: Centre for Climate Research Singapore, Singapore.

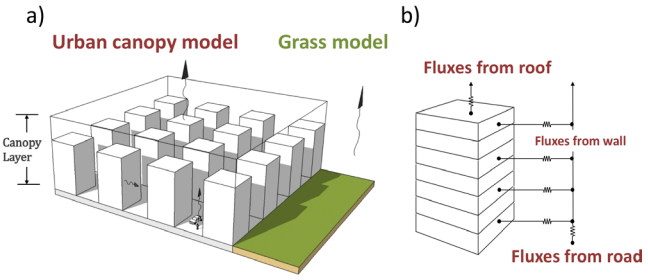

Fig. 1. Structure of the MUCM. (a) The canopy layer contains an infinite array of identical buildings and roads. (b) At each vertical layer, the fluxes are calculated for each urban surface, such as from the four walls of each building.

model considers grass or vegetation land as a bulk layer with the appropriate thermal conductivity, heat capacity, roughness length, and albedo. The latent heat exchange between the surface and the atmosphere above is solved using the Bowen method. The total fluxes from the surface are calculated as weighted average of fluxes from urban and vegetation fractions.

2.1 Governing equation

The MUCM is represented by single-column diffusion equations for momentum, potential temperature, and specific humidity. Drag terms are added to the momentum equations to represent air friction with the buildings. Also, sensible and latent heat source terms are added to the potential temperature and specific humidity equations to represent the heat flux exchange between the building walls and the air. The resulting equations, shown below, are consistent with those of Kondo et al. (2005).

$$\frac{\partial u}{\partial t}=\frac{1}{m}\frac{\partial}{\partial z}\left(K_m m\frac{\partial u}{\partial z}\right)+f(v-v_g)-c_d A u(u^2+v^2)^{1/2} \tag{1}$$

$$\frac{\partial v}{\partial t}=\frac{1}{m}\frac{\partial}{\partial z}\left(K_m m\frac{\partial v}{\partial z}\right)-f(u-u_g)-c_d A v(u^2+v^2)^{1/2} \tag{2}$$

$$\frac{\partial \theta}{\partial t}=\frac{1}{m}\frac{\partial}{\partial z}\left(K_h m\frac{\partial \theta}{\partial z}\right)+\frac{Q_{AS}}{\rho c_p} \tag{3}$$

$$\frac{\partial q_v}{\partial t}=\frac{1}{m}\frac{\partial}{\partial z}\left(K_q m\frac{\partial q_v}{\partial z}\right)+\frac{Q_{AL}}{\rho l} \tag{4}$$

Here, u and v are the wind velocity components, u_g and v_g are the geostrophic wind components, θ is the potential temperature, q_v is the specific humidity, f is the Coriolis parameter, m is the volume porosity (Kondo et al. 2005), c_d is the drag coefficient, ρ is the air density, and l is the latent heat of evaporation being assumed constant. Q_{AS} and Q_{AL} are the sensible and the latent heat fluxes from the building's surfaces to the atmosphere at each vertical layer of the model, respectively. K_m, K_h, and K_q are the turbulence diffusivities for momentum, heat, and water vapor, respectively, which are calculated using the Mellor–Yamada scheme level 2 (Mellor and Yamada 1974). The parameter $A = b/[(b + w)^2 - b^2]$, where b is building width and w is canyon width. According to Kondo et al. (2005) the volume porosity m is defined as

$$m=1-\left[\frac{b^2}{(b+w)^2}\right]P_b(z) \tag{5}$$

where $P_b(z)$ is the building density distribution with $0 < P_b(z) < 1$, $P_b(z) = 0$ means no building at level z, and $P_b(z) = 1$ means fully occupied by buildings.

The heat budget equation is solved for each urban surface i to compute the net radiation heat-flux exchange $Rnet_i$ between surface i and the atmosphere:

$$Rnet_i = H_i + lE_i + G_i, \tag{6}$$

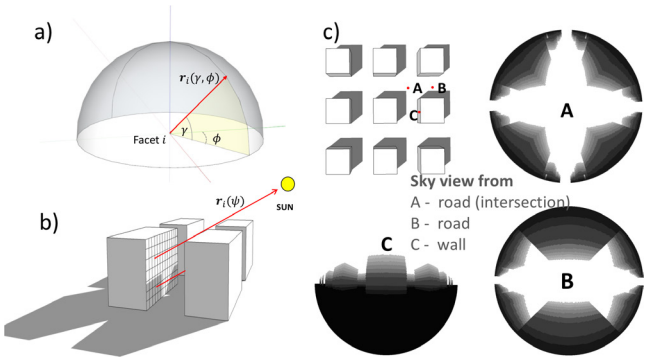

Fig. 2. Determining the view factors and sunlit fraction. (a) Generating a ray from a point on urban surface i. (b) Ray toward the sun from a pixel on urban surface i. (c) View from points on road A and B, and from wall C. Fading gray colors indicate view to different urban vertical layers.

where H_i is the sensible heat flux, lE_i is the latent heat flux, and G_i is the conductive heat flux at urban surface i. The sensible and latent heat fluxes at the road and the building roof are calculated using the Monin-Obukhov similarity method (Monin and Obukhov 1954), whereas those from wall surfaces are calculated from the Jurges formula. The conductive heat flux G is calculated using one-dimensional thermal-conduction equation

$$G=-\lambda\frac{\partial T_x}{\partial x} \quad \text{and} \tag{7}$$

$$\frac{\partial T_x}{\partial t}=\frac{1}{\rho c}\frac{\partial G}{\partial x}, \tag{8}$$

where λ is the heat conductivity, T_x is the interior temperature at depth x of the urban material, and pc is volumetric heat capacity of the material.

2.2 Ray tracing algorithm

A difference between our MUCM and other multi-layer models is the use of a ray-tracing algorithm to estimate view factors and sunlit areas of urban surfaces. Essentially, the algorithm traces the path of light, and then simulates the way that the light interacts with the visual objects.

Consider the view factors. In radiative heat transfer, a view factor $F_{i\to j}$ from surface i to surface j is defined as the fraction of the radiation leaving i that strikes j. The procedure to calculate $F_{i\to j}$ is as follows:

(1) Send out rays from an origin point on surface i. The origin point is defined as the middle point of surface i and a given ray $\boldsymbol{r}_i(\gamma, \phi)$ travels in the direction defined by angles γ and ϕ (see Fig. 2a).
(2) Determine if the ray strikes surface j. Define $l_i(\gamma, \phi) = 1$ if ray $\boldsymbol{r}_i(\gamma, \phi)$ intersects with surface j, otherwise $l_i(\gamma, \phi) = 0$.
(3) Count the number of the rays striking surface j. $F_{i\to j}$ equals the number of rays hitting surface j divided by the total number of rays leaving surface i. Thus,

$$F_{i\to j}=\frac{1}{N_i}\sum_{k=1}^{N_i} I_{i\to j}(\gamma_k,\phi_k) \tag{9}$$

$$F_{i\to s}=1-\sum_{j=1}^{N_s} F_{i\to j}, \tag{10}$$

where N_i is the total number of rays leaving i. Also shown above in Eq. (10) is the sky view factor $F_{i\to s}$ from surface i, which is simply defined as 1 minus the total view factors from i to all N_s surfaces.

To calculate sunlit fraction of a surface, we use a similar method:

(1) Divide urban surface i into pixels (see Fig. 2b). Assume sur-

face i has N_p pixels.

(2) From the middle point of each pixel ψ on surface i, draw a ray $\boldsymbol{r}_i(\psi)$ toward the sun, knowing the solar elevation and azimuth angle.

(3) Determine if the ray intersects with any other surfaces within the urban canopy. Define $l_{i\to o}(\psi) = 1$ if ray $\boldsymbol{r}_i(\psi)$ hits any objects on its path, otherwise, $l_{i\to o}(\psi) = 0$.

(4) The sunlit fraction on surface i is obtained as 1 minus the fraction of rays hitting objects to the number of pixels (Eq. 11).

$$S_i = 1 - \frac{1}{N_p}\sum_{\psi=1}^{N_p} I_{i\to o}(\psi) \tag{11}$$

3. Model testing

We now test the MUCM against measured data in Kugahara, Tokyo (139.84°E, 35.83°N) on 1 September 2005. The data, provided by the Kugahara project (Moriwaki and Kanda 2004; Moriwaki et al. 2006), include near-ground and vertical profiles measured by instruments attached to a 29-m tower (Fig. 3 and Table 1). Figure 4 shows the diurnal cycle of input variables. The wind velocity at 29 m, as well as the air temperature and specific humidity at 28 m, are used as the upper boundary condition. Downward shortwave and longwave radiative fluxes at 25 m are used as input data. Note that there is a sharp decrease in wind velocity around 9 am at Kugahara. The same decrease was also seen in the wind data observed at multiple nearby AMeDAS (Automated Meteorological Data Acquisition System) stations, such as Tokyo and Haneda, implying it was possibly due to the change of a larger weather system during that time. The anthropogenic heat flux is provided at the bottom layer comes from Ikeda and Kusaka (2010). The data was originally estimated by Mizuno et al. (1997), but being updated to 2006 (Ikeda and Kusaka 2010).

Kugahara is a residential area of Tokyo, Japan, that consists of densely packed, low-storied houses of average height 7.3 m, paved roads, and small playgrounds. The vegetation fraction of the area is about 20.6% and the building fraction is about 32.6% (Moriwaki and Kanda 2004). Urban thermal parameters such as heat capacity, thermal conductivity, albedo, and the roughness length of the buildings and roads are adapted to the local condition. The model simulated four days under the atmospheric conditions of 1 September 2005, and we use the results from the 4th day to compare to observation.

Consider the diurnal cycle of the simulated near-surface temperature. Figure 5 shows good agreement between the simulated and observed data except for a small overestimate of peak daytime and nighttime temperatures. The vertical profiles of temperature also show good agreement with observations (Fig. 6a). On the other hand, the model overestimates the windspeed at the lower levels during the daytime (Fig. 6b), a result that may be due to an underestimate of the building drag effect. On the other hand, the

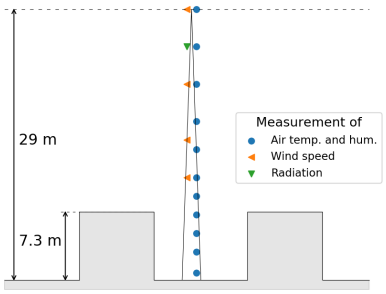

Fig. 3. Placement of measuring instruments of air temperature, humidity, wind speed and radiation.

Table 1. Measurement positions and landcover fractions for model comparison. Heights are in meters.

Location	Kugahara, Tokyo, Japan (35.835°N, 139.842°E)
Landcover	Low-storied residential; Fraction of building: 32.6%, vegetation: 20.6%; Building height: 7.3
Height of measurements of wind	29, 21, 15, 11
Height of measurements of air temperature and humidity	0.75, 3, 5, 7, 9, 11, 14, 17, 21, 25, 29
Height of measurement of radiation.	25

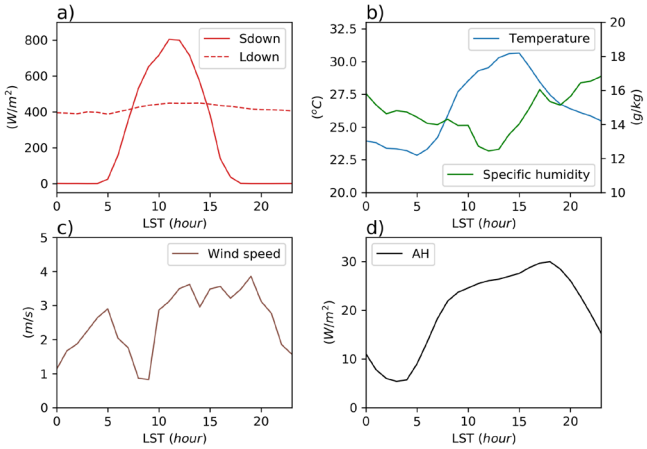

Fig. 4. Measurements at Kugahara, Tokyo, on 1 September 2005. (a) Total downward solar radiation Sdown and downward longwave radiation Ldown. (b) Temperature and specific humidity. (c) Windspeed at 29 m. (d) Anthropogenic heating. LST is an abbreviation for Local Standard Time.

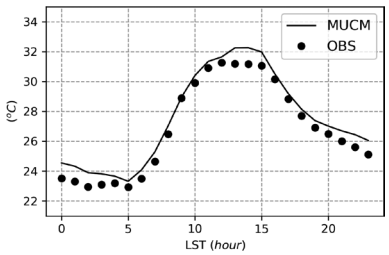

Fig. 5. Diurnal cycle of simulated air temperature at 0.75 m versus observation.

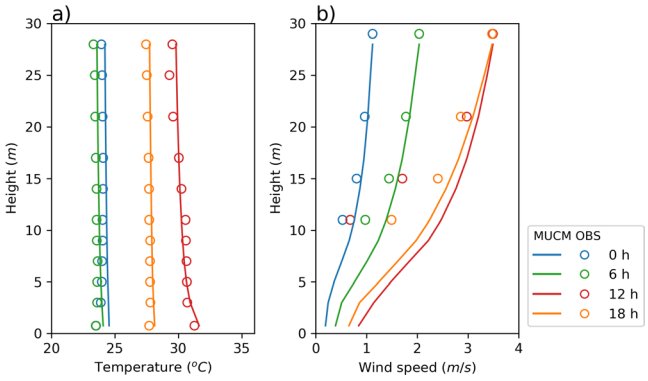

Fig. 6. Vertical profiles of the simulated and observed air temperature and windspeed at various times. (a) Temperature. (b) Windspeed. The times are local times.

Table 2. Computational times of the component schemes of the model.

Task	Time needed
Total run	9.45 sec
Surface scheme (includes MUCM and simple grass model).	6.79 sec
Ray-tracing scheme	0.82 sec

validation of solar radiation within the urban canopy layer has not done due to the limitation of measured data collected. This issue will be addressed in a further work.

The simulation run time was tracked to estimate the computational cost of the ray-tracing scheme in relation to the total cost. The resulting times in Table 2 show that the model needed 9.45 sec to finish the testing run, whereas the surface scheme took 6.79 sec and the ray-tracing scheme 0.82 sec with N_i, N_s, and N_p being 7200, 160 and 10, respectively. Thus, the time for the ray-tracing scheme is about 12% of the surface scheme and about 9% of the total model time. We conclude that the ray-tracing scheme is not too computationally costly compared with the total run time.

4. Summary

This study introduced a new multiple-layer urban canopy model combined with a forward ray-tracing algorithm. The model parameterizes urban morphology as an infinite array of buildings and roads, with the buildings being identical right-square prisms. The ray-tracing scheme is coupled to the model to calculate the view factors and sunlit fractions on each urban surface at each vertical layer. The scheme allows the explicit representation of radiative flux exchange between urban surfaces and between the surfaces and the sun. The model was tested against observations at Kugahara, Tokyo, with the result showing good performance of the model for both the diurnal cycle of the surface air temperature and the vertical profiles of air temperature and windspeed.

For this simulation, the computational cost of the ray-tracing scheme was found to be small, spending only 0.82 sec on the ray tracing scheme, corresponding to 9% of the total run time of 9.45 sec and only 12% of total time for the surface scheme. Thus, the ray-tracing scheme appears to have a relatively low computational cost.

Although the newly proposed model was validated against observation, we have not yet determined whether the ray-tracing scheme can improve the representation of radiative exchanges within urban canopy layer. This issue may be addressed in subsequent work.

Acknowledgments

This research was supported by a Grant-in-Aid for Scientific Research B (18H00763) of the Japan Science and Technology Agency (JST), Japan.

Edited by: S. Nishizawa

References

Aoyagi, T., and N. Seino, 2011: A square prism urban canopy scheme for the NHM and its evaluation on summer conditions in the Tokyo metropolitan area, Japan. *J. Appl. Meteor. Climatol.*, **50**, 1476−1496.

Best, M. J., 2005: Representing urban areas within operational numerical weather prediction models. *Bound.-Layer Meteor.*, **114**, 91−109.

Brown, M. J., 2000: Urban parameterizations for mesoscale meteo- rological models. *Mesoscale Atmospheric Dispersion*, Z. Boybeyi, Ed., Wessex Press, 193−255.

Dupont, S., T. L. Otte, and J. K. S. Ching, 2004: Simulation of meteorological fields within and above urban and rural canopies with a mesoscale model. *Bound.-Layer Meteor.*, **113**, 111−158.

Grimmond, C. S. B., and co-authors, 2010: The international urban energy balance models comparison project: First results from Phase 1. *J. Appl. Meteor. Climatol.*, **49**, 1268−1292.

Grimmond, C. S. B, and co-authors, 2011: Initial results from Phase 2 of the international urban energy balance model comparison. *Int. J. Climatol.*, **31**, 244−272.

Hagishima, A., J. Tanimoto, T. Katayama, and K. Ohara, 2001: An organic analysis for quantitative estimation of heat island by the revised architecture-urban-soil-simultaneous simulation model, AUSSSM. Part 1: Theoretical frame of the model and results of standard solution. *J. Archit. Plann. Environ. Eng.*, **550**, 79−86 (in Japanese).

Harman, I. N., J. F. Barlow, and S. E. Belcher, 2004: Scalar fluxes from urban street canyons. Part II: Model. *Bound.-Layer Meteor.*, **113**, 387−410.

Ikeda, R., and H. Kusaka, 2010: Proposing the simplification of the multilayer urban canopy model: Intercomparison study of four models. *J. Appl. Meteor. Climatol.*, **49**, 902−919.

Kanda, M., T. Kawai, M. Kanega, R. Moriwaki, K. Narita, and A. Hagishima, 2005a: A simple energy balance model for regular building arrays. *Bound.-Layer Meteor.*, **116**, 423−443.

Kanda, M., T. Kawai, and K. Nakagawa, 2005b: A simple theoretical radiation scheme for regular building arrays. *Bound.-Layer Meteor.*, **114**, 71−90.

Kondo, H., Y. Genchi, Y. Kikegawa, Y. Ohashi, H. Yoshikado, and H. Komiyama, 2005: Development of a multi-layer urban canopy model for the analysis of energy consumption in a big city: Structure of the urban canopy model and its basic performance. *Bound.-Layer Meteor.*, **116**, 395−421.

Krayenhoff, E. S., and J. A. Voogt, 2007: A microscale three-dimensional urban energy balance model for studying surface temperatures. *Bound.-Layer Meteor.*, **123**, 433−461.

Kusaka, H., H. Kondo, Y. Kikegawa, and F. Kimura, 2001: A simple single-layer urban canopy model for atmospheric models: Comparison with multi-layer and slab models. *Bound.-Layer Meteor.*, **101**, 329−358.

Lee, S.-H., and S.-U. Park, 2008: A vegetated urban canopy model for meteorological and environmental modeling. *Bound.-Layer Meteor.*, **126**, 73−102.

Martilli, A., A. Clappier, and M. W. Rotach, 2002: An urban surface exchange parameterisation for mesoscale models. *Bound.-Layer Meteor.*, **104**, 261−304.

Masson, V., 2000: A physically-based scheme for the urban energy budget in atmospheric models. *Bound.-Layer Meteor.*, **94**, 357−397.

Mellor, G. L., and T. Yamada, 1974: A hierarchy of turbulence closure models for planetary boundary layers. *J. Atmos. Sci.*, **31**, 1791−1806.

Mizuno, T., and co-authors, 1997: Development of a verification method of warming provision technologies within metropolitan cities. *National Institute for Resources and Environment Rep.*, 97-1, 311 pp (in Japanese).

Monin, A. S., and A. M. F. Obukhov, 1954: Basic laws of turbulent mixing in the surface layer of the atmosphere. *Contrib. Geophys. Inst. Acad. Sci. USSR*, **151**, e187.

Moriwaki, R., and M. Kanda, 2004: Seasonal and diurnal fluxes of radiation, heat, water vapor, and carbon dioxide over a suburban area. *J. Appl. Meteor.*, **43**, 1700−1710.

Moriwaki, R., and M. Kanda, 2006: Flux-gradient profiles for momentum and heat over an urban surface. *Theor. Appl. Climatol.*, **84**, 127−135.

Oleson, K. W., G. B. Bonan, J. Feddema, M. Vertenstein, and C. S. B. Grimmond, 2008: An urban parameterization for a global climate model. Part I: Formulation and evaluation for two cities. *J. Appl. Meteor. Climatol.*, **47**, 1038−1060.

Otte, T. L., A. Lacser, S. Dupont, and J. K. S. Ching, 2004: Implementation of an urban canopy parameterization in a meso-scale meteorological model. *J. Appl. Meteor.*, **43**, 1648−1665.

Salamanca, F., A. Krpo, A. Martilli, and A. Clappier, 2010: A new building energy model coupled with an urban canopy parameterization for urban climate simulations—Part I. Formulation, verification, and sensitivity analysis of the model. *Theor. Appl. Climatol.*, **99**, 331.

Vu, C. T., Y. Ashie, and T. Asaeda, 2002: A k-ε turbulence closure model for the atmospheric boundary layer including urban canopy. *Bound.-Layer Meteor.*, **102**, 459−490.

Warner, T. T., 2011: *Numerical Weather and Climate Prediction*. Cambridge University Press, 171−196. doi:10.1017/CBO9780511763243.

Manuscript received 8 January 2019, accepted 10 January 2019
SOLA: https://www.jstage.jst.go.jp/browse/sola/